Heliyon 6 (2020) e05464

Contents lists available at ScienceDirect

Heliyon

journal homepage: www.cell.com/heliyon

Research article

Experimental approach, theoretical investigation and molecular docking of 2- chloro-5-fluoro phenol antibacterial compound

V. Vidhya [a], A. Austine [b], M. Arivazhagan [c,*]

[a] Department of Physics, Trichy Engineering College, Affiliated to Bharathidasan University, Tiruchirappalli, Tamilnadu, India
[b] PG&Research Department of Physics, Periyar E.V.R College, Affiliated to Bharathidasan University, Tiruchirappalli, Tamilnadu, India
[c] PG&Research Department of Physics, Government Arts College, Affiliated to Bharathidasan University, Tiruchirappalli, Tamilnadu, India

ARTICLE INFO

Keywords:
DFT
Dimer
NLO
Antibacterial activity
Molecular docking
Computational materials science
Materials characterization
Structural analysis
Structural behavior
Computational chemistry
Organic chemistry
Molecular modeling
Pharmaceutical chemistry
Microbiology
Pharmaceutical science

ABSTRACT

The molecular structural dimerization of biologically potent 2-chloro-5-fluoro phenol (2C5FP) is optimized. A combined experimental and theoretical characteristics of vibrational spectral determinations (NMR, FT-IR and Raman) on 2-chloro-5-fluoro phenol (2C5FP) were used at DFT-B3LYP/6–31++G (d,p) level of computation. A close coherence is achieved when experimentally observed wave numbers are compared with calculated wave numbers by refinement of the scale factors. Calculated values of global chemical descriptors of the present molecule reveal significant molecular stability and chemical reactivity. Non-Linear optical (NLO) property of the present molecule is investigated by determining the second order non linear parameter of first hyperpolarizability β. Moreover, hydrogen bond and thermodynamic parameters at various temperatures are determined and discussed. Investigated compound 2C5FP possesses a better antibacterial activity against *Echerichia* coli, *Streptococcus aureus, Pseudomonas aureus*,and *Staphylococcus aureus*, respectively. The title molecule is subjected to molecular docking studies with two different proteins, namely *Staphylococcus aureus* Tyrosyl-tRNA synthetase (PDB ID: 1JIL) and human dihydroorotate dehydrogenase (hDHODH) (PDB ID: 6CJF). The results of molecular docking analysis support the antibacterial activity and demonstrate a strong interaction with the DHODH inhibitor.

1. Introduction

The antioxidant potential of phenolic compounds exhibit potent activities in the treatment of cancer. These compounds are considered as secondary metabolities, which are most significant bioactive agent in chemo preventive and chemotherapeutic effects in cancer [1]. Phenolic compounds, ubiquitous in edible plants like, flavonoids, chromones, tanins, lignans, quinines, phenolic acids and many more. Polyphenols have reported to many industrial applications. For instance, they can be used as natural colorants, food preservatives and in the production of paints, paper and cosmetics [2]. One of the most important polyphenolic flavonoids found in fruits and vegetables [3] (Apple, grapes, tomato, green tea pine and many others) act as an antioxidants due to their redox potential possessing anticancer activities on different cancer cell lines as in, MCF-7 breast cancer and HeLa cervical cancer cells, A549 lung cancer cell, Miapaca-2, Panc-1 and SNU-213 human pancreatic cancer cells [4]. More than 20 phenols were investigated that displayed inhibitory activities of the β-class carbonic anhydrase from the fungal parasite *Malassezia globosa* (MgCA). All tested phenols exhibited better efficacy in inhibiting MgCA than the clinically used sulfonamide acetazolamide [5]. In particular, when humans regularly consume high levels of fresh fruits and vegetables, flavonoids have been associated with prevention of cancer and heart diseases. Phenyl sulfonylfuroxan NO-donor phenols are preventive agents for metabolic syndrome since metabolic syndrome (Mets) give rise to dyslipidemia, raised fasting glucose, renal and liver diseases, for the development of cardiovascular diseases (CVD) and type-2 diabetic mellitus (T2DM) [6].

The hydroxyl group of aromatic ring from the phenolic compounds displays antimicrobial, anti-artherogenic, anti-inflammatory, cytotoxic, and pharmacological activities [7], respectively. Flavonoids, consisting of two aromatic rings A and B, joined by a 3-carbon bridge have low molecular weight compounds with fifteen carbon atoms arranged in

* Corresponding author.
E-mail address: jjmarivu@yahoo.co.in (M. Arivazhagan).

https://doi.org/10.1016/j.heliyon.2020.e05464
Received 1 October 2020; Received in revised form 3 November 2020; Accepted 4 November 2020
2405-8440/© 2020 Published by Elsevier Ltd. This is an open access article under the CC BY-NC-ND license (http://creativecommons.org/licenses/by-nc-nd/4.0/).

C6-C3-C6 configuration [2]. Flavonoids are commonly found in phytochemicals which can be used to protect the plant against UV light, herbivores, fungal parasites, oxidative cell injury and hypo lipidemic [8]. Due to low toxicity fluorine derivatives of phenols have wide variety of applications in agricultural chemicals, dyes biocides and potential therapy of skin disorders [9], respectively. Chlorophenols used for many applications in the photochemical industry is due to the substituted donor (OH) and acceptor (CL) group of atoms in the benzene ring [10].

Considering the above remarkable significant applications of phenol derivatives in pharmaceutical industry, the antibacterial activity and molecular docking have been reported for title compound 2-chloro-5-fluoro phenol. The vibrational spectroscopic studies of various phenol derivatives have been reported in earlier literatures [11, 12]. N. Sunderaganesan *et. al* and D. Mahadevan *et. al* were investigated the vibrational analysis of 2,3- difluoro phenol and 3- bromo phenol [13, 14]. The substitution of halogen atoms on the title compound influences the drug activity and binding affinity by molecular docking. The previous study reports that the spectroscopic investigations and DFT studies of 2-chloro-5-fluoro phenol have not been reported so far. Hence, detailed theoretical studies and an extensive experimental investigation on IR, Raman and NMR spectra of the title molecule have been performed. Besides, intra and intermolecular hydrogen bond interaction, global chemical parameters are determined from HOMO-LUMO energy gap and NLO activities of the title compound have been carried out. Finally, due to potential biological activities of 2C5FP molecule is subjected to antibacterial activity.

2. Materials and methods

2.1. Experimental

The fine sample 2C5FP was procured from Lancaster chemical company, UK. The FT-IR spectrum was recorded in BRUKER IFS 66V spectrometer and FT-Raman spectrum was recorded using FRA-106 Raman module equipped with Nd: YAG Laser source operating at 1.064μm width with 200mW power. Both FT-IR and FT-Raman spectra were measured in the region of 4000–100cm^{-1} and 3500-100cm^{-1}, respectively. The spectral wave numbers of all bands are accurate to ± cm^{-1}. The carbon and proton (^{13}C & ^{1}H) NMR spectra were recorded in Acetone using TMS as an internal standard on Bruker NMR spectrometer at 400 MHz. The spectral measurements were recorded at IIT (SAIF), Chennai, India.

2.2. Antibacterial activity

The isolates of bacterial strains viz, *Streptococcus aureus, Staphylococuss aureus,* (Gram – positive bacteria), *Escherichia coli* and *Pseudomonas aureus* (Gram – negative bacteria) were obtained from the Department of Microbiology, Srimad Andavan College, Trichy, Tamilnadu, India.

2.2.1. Disc diffusion method

The antibacterial activity of the title compound 2C5FP is performed by the *in-vitro* disc diffusion technique described by Kirby and Bauer [15]. The antibacterial activity is determined over the active compound (2C5FP) against two gram – positive isolates and against two gram – negative isolates. In the disc diffusion method, the compound solution was prepared by dissolving the test compound (2C5FP) in 90% ethylene in the concentration of 1 mg/ml. The sterile paper discs with 6mm in diameter loaded with test compound were placed in test bacteria spread agar plates. The bacterial plates are incubated at 37 °C [16, 17]. Standard antibiotic amoxicillin was used as positive control with concentration of 1 mg/ml. The results obtained for the tested compound as the average diameter of inhibition zone of bacterial growth around the discs in mm after 24h incubation period.

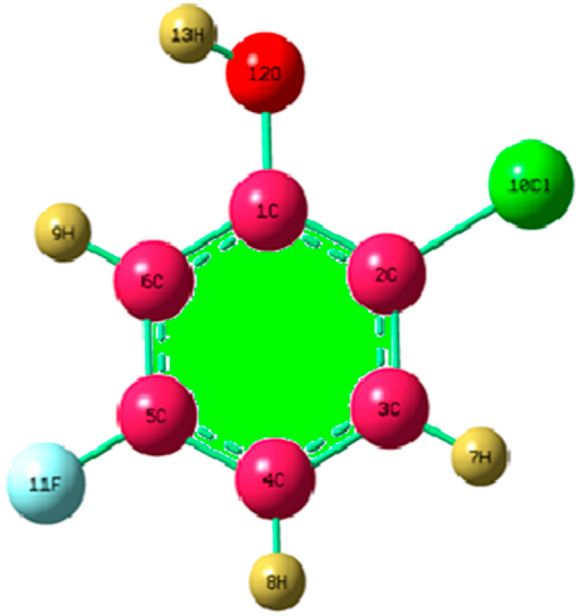

Figure 1. Monomer structure of 2-chloro-5-fluoro phenol.

2.3. Methods of computation

All Computations were accomplished with Gaussian 09 software package of programs for the title compound using DFT with Becke's three parameter exchange functional in combination with the Lee-Yang-Parr correlation functional (B3LYP) with standard 6–31++G (d, p) level of computations. In order to minimize the energy, the geometric optimization was performed along with all geometrical parameters without imposing molecular symmetric constraints. After geometric optimization, the vibrational assignments were made on the basis of potential energy distributions using MOLVIB Program (version V7.0-G77) written by Sundis [18, 19]. Calculated theoretical wave numbers were quite close to experimental wave numbers when they were scaled using MOLVIB. The scale factors were determined using linear correlation method between the theoretical and experimental fundamental modes. The global chemical indices namely ionization potential, electron affinity, hardness, softness, chemical potential, and electrophilicity index have been obtained from HOMO-LUMO analysis performing at B3LYP/6–31++G (d, p) basis set.

2.3.1. Molecular docking

The crystal structures of *staphylococcus aureus* tyrosyl-tRNA synthetase (PDB ID: 1JIL) and the hDHODH inhibitor (PDB ID: 6CJF) are downloaded from the RSCB Protein Data Bank (PDB). The optimized molecular structure using DFT is useful to prepare the ligand PDB format. The ligand is prepared by minimizing the energy at B3LYP/6–31++G (d,p) level of computation. The protein is prepared by eliminating the water, co-factors and co-crystalline ligands. By using the Auto Dock Tools (ADT) graphical user interface is used to compute the Kollman charges and polar hydrogen. The bioactive confirmation is simulated using Autodock 4.2 software package and the corresponding results are analyzed using PyMol software [20, 21]. Partial charges are computed by Gasteiger method and the receptor grids are generated using 90 × 90 × 90 A^{0} grid points in XYZ coordinates.

Table 1. Calculated structural parameters of 2-Chloro-5-fluoro phenol at B3LYP/6–31++G (d,p) method.

Bond Length (A^0)

Parameters	Monomer	Dimer	Exp[a]
C1-C2	1.41	1.41	1.41
C1-C6	1.40	1.40	1.38
C1-O12	1.36	1.35	1.38
C2-C3	1.39	1.39	1.41
C2-Cl10	1.75	1.75	1.74
C3-C4	1.40	1.40	1.42
C3-H7	1.08	1.08	1.09
C4-C5	1.39	1.39	1.04
C4-H8	1.08	1.08	1.09
C5-C6	1.39	1.39	1.38
C5-F11	1.36	1.36	-
C6-H9	1.09	1.09	1.09
O12-H13	0.97	0.97	0.99
O12-H26	-	1.99	-
O25-H13	-	1.99	-

Bond Angle (°)

Parameters	Monomer	Dimer	Exp[a]
C2-C1-C6	119.24	118.92	118.0
C2-C1-O12	118.36	118.57	118.0
C6-C1-O12	122.40	122.51	124.0
C1-C2-C3	120.28	120.56	121.0
C1-C2-Cl10	119.70	119.60	-
C3-C2-Cl10	120.02	119.83	-
C2-C3-C4	120.91	120.82	120.0
C2-C3-H7	118.97	119.02	-
C4-C3-H7	120.12	120.14	-
C3-C4-C5	117.76	117.65	119.0
C3-C4-H8	121.72	121.77	-
C5-C4-H8	120.51	120.58	-
C4-C5-C6	122.83	123.03	123.0
C4-C5-F11	119.13	118.93	-
C6-C5-F11	118.04	118.05	-
C1-C6-C5	118.98	119.00	117.0
C1-C6-H9	121.23	120.87	-
C5-C6-H9	119.79	120.13	-
C1-O12-H13	110.13	111.12	

Dihedral Angle (°)

Parameters	Monomer	Dimer
C6-C1-C2-C3	0.0	0.0
C6-C1-C2-Cl10	180	-180
O12-C1-C2-C3	180	180
O12-C1-C2-L10	0.0	-0.1
C2-C1-C6-C5	0.0	0.0
C2-C1-C6-H9	-180	-180
O12-C1-C6-C5	180	-180
O12-C1-C6-H9	0.0	0.5
C2-C1-O12-H13	180	-179.09
C6-C1-O12-H13	180	-138.17
C1-C2-C3-C4	180	-0.07
C1-C2-C3-H7	0.0	180
CL10-C2-C3-C4	0.0	180
CL10-C2-C3-H7	180	-0.1

[a] Refs. [13, 14, 20].

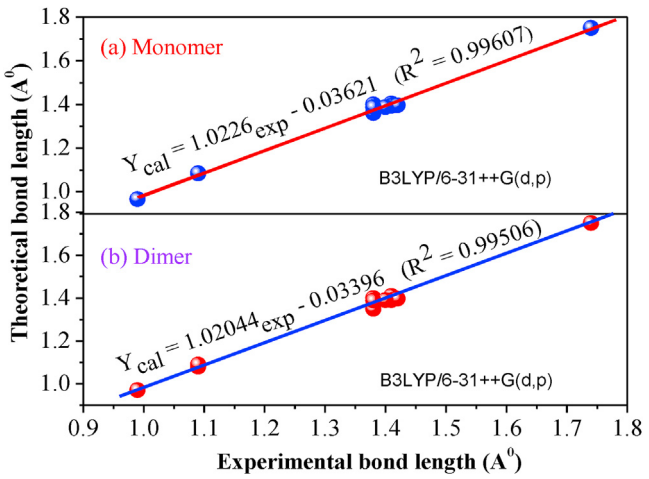

Figure 2. Correlation graphic between experimental and calculated bond lengths of 2-chloro-5-fluoro phenol (a) Monomer (b) Dimer.

3. Result and discussion

3.1. Molecular geometry

The optimized monomer and dimer structure of present compound 2C5FP is obtained from GAUSSIAN 09W program package. The optimized structure of monomer is shown in Figure 1. Comparative optimized structural parameters such as bond length and bond angle for two different conformers of title molecule is performed using B3LYP method 6–31++G (d, p) basis set as summarized in Table 1. Theoretical results demonstrate that most of the bond lengths and bond angles of monomer and dimer structure are well consistent with the similar theoretical and XRD data reported earlier [13, 14]. The calculated results show that the aromatic ring of the title molecule is perturbed from the regular hexagon as a result of the electronic effects of chloro, fluoro and bromo group. This leads to variation in the charge distribution on the carbon atom of the benzene ring and consequently causes the structural, vibrational and electronic properties of the molecule. In addition, the sharing of π electrons between the oxygen atom from OH group and electro negativity of fluorine and chlorine atoms affects the structural perturbations within the ring. Calculated bond lengths and bond angles are slightly overestimate in the bond lengths of C1-C6, C1-O12, C2-Cl10, C5-C6 and bond angles of C2-C1-C6, C1-C6-C5 & C2-C3-C4. A small reduction is observed in the bond length of C1-O12, C2-C3, C3-C4, C3-H7, C4-H8, O12-H13 and bond angles of C6-C1-O12 & C1-C2-C3 when compared with XRD values [22]. These small deviations between observed and calculated entities are obtained from different environments. It is evident that the experimental predictions belong to solid phase and theoretical results belong to gaseous phase.

The variation in bond lengths and bond angles depends on the substitution of electron withdrawing and electron donating groups in the benzene ring and various factors such as hybridization, size of the atoms,

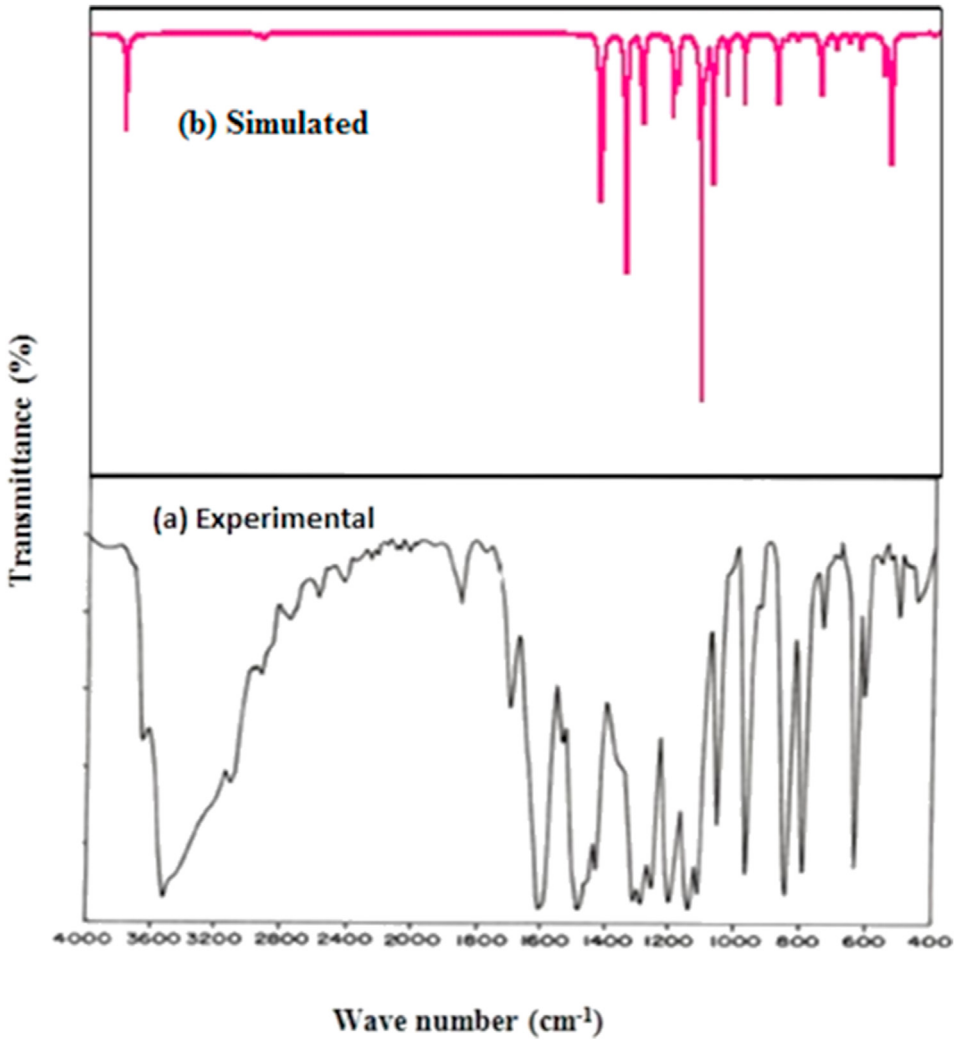

Figure 3. Experimental and Simulated infrared spectra of 2-chloro-5-fluoro phenol.

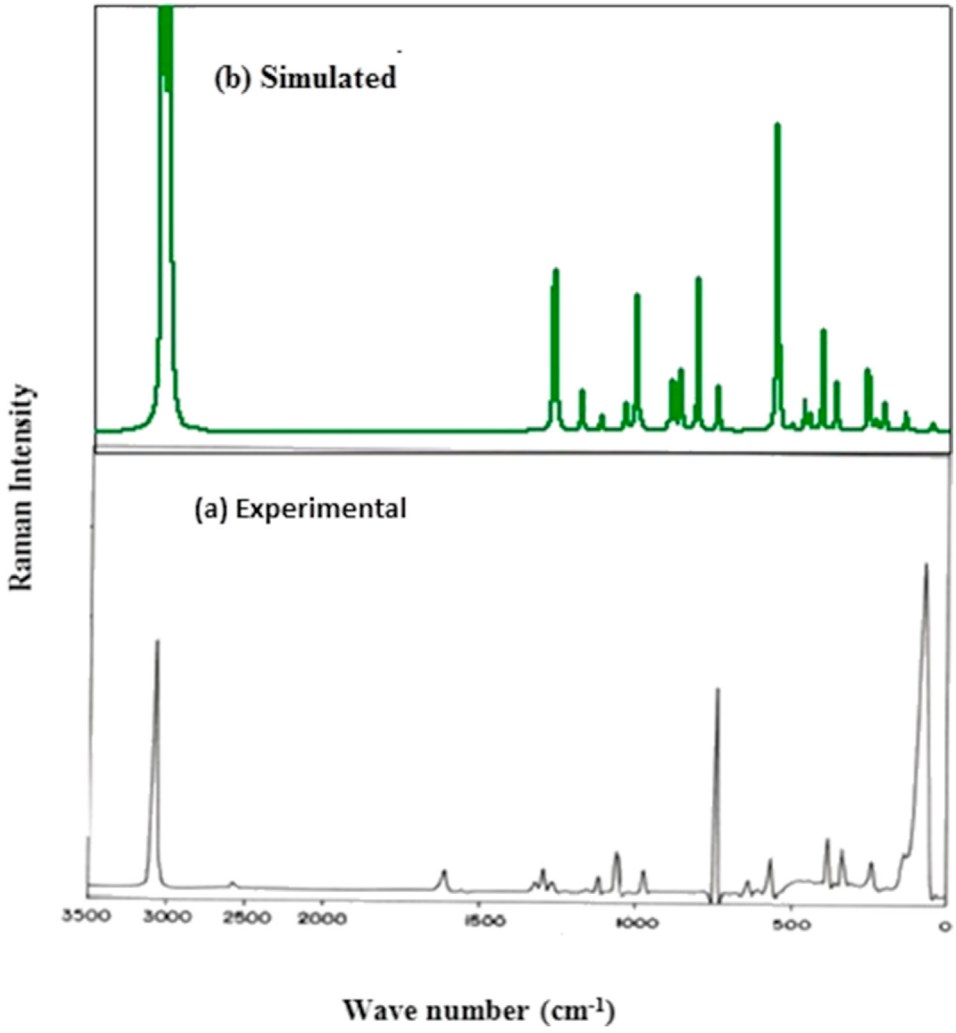

Figure 4. Experimental and Simulated Raman spectra of 2-chloro-5-fluoro phenol.

delocalization of electrons, lone pair of electrons and electro negativity difference between the atoms. For instance, the bond length of C2-Cl10 (1.75A^0) is greater than the bond length of C5-F11 (1.36 A^0) which reveals that the size of the atoms increases as bond length increases. The C-X (X = F, Cl, Br...) bond distance denotes a considerable rising when substituted in the benzene ring in the place of C-H. In the title molecule, bond lengths of C-Cl and C-F nearly well coincides with 1.75 A^0 and 1.36 A^0 which is in good coherence with calculated value in the earlier literature for P-chlorophenol and 2,3-difluoro phenylboronic acid, respectively [23, 24]. A remarkable reduction observed in the bond angle of C1-O12-H13 (110.13 A^0) is due to the presence of a lone pair of electrons in the central oxygen atom.

The linearity between the observed and computed bond lengths and bond angles of monomer and dimer structure of 2C5FP can be estimated from plotting the computed data against experimental ones which is depicted in Figure 2 and are described through the following equations.

$$Y_{Cal} = 1.0226\ _{Exp} - 0.03621\ (R^2 = 0.99607) \text{ for Monomer} \quad (1)$$

$$Y_{Cal} = 1.02044\ _{Exp} - 0.03396\ (R^2 = 0.99997) \text{ for Dimer} \quad (2)$$

3.2. Interpretations of fundamental modes

According to theoretical computations, 2-chloro-5-fluoro phenol (2C5FP) has a planar structure with 13 atoms and 33 fundamentals modes of vibration along with C1 point group symmetry. The comparisons of observed and simulated FT-IR and FT Raman spectra of 2C5FP are shown in Figures 3 and 4, respectively. In the present investigation, the vibrational assignments were predicted on the basis of potential energy distribution (PED) results have been carried out from the MOLVIB [19, 25] output. Table 2 reported the complete vibrational analysis performed at 6–31++G (d,p) basis set.

3.2.1. C-O & O-H vibration

The C-O stretching vibrations in P-mono substituted phenols observed as a strong band in the region 1300-1200cm^{-1} [26]. The C-O stretching band coupled with C-C stretching modes vibration. In the present compound, the C-O stretching mode is identified at 1258cm^{-1} in the FT-IR spectrum. The C-O in-plane and out-of-plane modes are identified within their characteristic region and the corresponding values are summarized in Table 2.

The O-H stretching modes are delicate to hydrogen bonding. A non-hydrogen bonded group absorbs strongly in the region 3700-3500cm^{-1}. In a five- and six-benzene ring compound, the presence of intra molecular hydrogen bond reduces the hydroxyl stretching mode to the 3559-3200cm^{-1} region. In the O-H region, due to the halogen substitution of the benzene ring stretching mode turns to the higher region. Accordingly in 2C5FP, the O-H stretching mode is found at 3524cm^{-1} in the FT-IR spectrum. This is well consistent with the

Table 2. Observed FT-IR, FT-Raman and calculated (unscaled and scaled) frequencies (cm^{-1}) of 2- Chloro-5-fluoro phenol at B3LYP/6-3 1++G (d,p) method.

S.NO	C1 Symmetry	Observed frequency		Calculated frequency		Assignment with PED %
		FT-IR	FT -Raman	Unscaled	Scaled	
1	A	3524	-	3829	3528	νOH (88)
2	A	3106	-	3233	3111	νCH (97)
3	A	-	3079	3216	3083	νCH (95)
4	A	2926	-	3201	2930	νCH (88)
5	A	1699	-	1657	1703	νCC (88) bOH 11
6	A	1607	1613	1641	1612	νCC (78) bCH 14
7	A	1536	-	1537	1540	νCC (70) bCH 16
8	A	1487	-	1459	1491	νCC (72) bCH 15
9	A	1316	1321	1362	1320	νCC (79) bOH 10
10	A	1292	1297	1317	1296	νCC(70) bCH 14
11	A	-	1267	1299	1274	bOH (76) bCH 11
12	A	1258	-	1193	1262	νCO(72) bCH (14)
13	A	1205	-	1172	1209	νCF(69) bCH (11)
14	A	1143	-	1135	1151	bCH (79) νCC (10)
15	A	1106	-	1071	1112	bCH (71)
16	A	1058	1059	991	1066	bCH (69)
17	A	970	974	941	984	ωCH (62)
18	A	933	-	840	942	ωCH (58)
19	A	850	-	806	861	ωCH (53)
20	A	796	-	751	803	bCCC (66)
21	A	-	743	693	751	bCCC (68)
22	A	729	-	642	733	νCCL (70) bCC (12)
23	A	696	-	619	702	bCCC (61)
24	A	638	641	568	647	bCO (66) ωCH (12)
25	A	610	-	512	617	bCF (61)bCCC(12)
26	A	564	570	459	581	ωCCC (56)
27	A	532	-	380	543	ωCCC (53)
28	A	508	-	348	519	ωCCC (48)
29	A	453		322	464	ωOH (52)
30	A	-	386	318	397	ωCO (45)
31	A	-	338	234	346	bCCL (51)
32	A	-	244	226	255	ωCCCF (49)
33	A	-	73	119	84	ωCCL (41)

Abbreviations: ν -stretching; b-in- plane bending; ω – out-of-plane bending.

literature data [23]. The O-H in-plane and out-of-plane bending modes are generally appeared in the region 1350-1200cm^{-1} and 720-590cm^{-1} [13], respectively. In 2C5FP, the O-H in-plane and out-of-plane vibrations are assigned at 1267cm^{-1} in FT-Raman and 453cm^{-1} in FT-IR, respectively.

3.2.2. C-H vibration

Aromatic compounds generally shows the multiple weak bands due to C-H stretching vibration in the region 3100-3000cm^{-1}. The C-H in-plane bending vibration coupled with C-C stretching modes which occur in the region 1500-1100cm^{-1} and C-H out-of-plane bending modes appear in the region 1000-800cm^{-1} [27]. In this region, the modes are not affected substantially by the substituents. Hence, in the present molecule of the FT-IR and Raman spectra the bands at 3106, 2926 and 3079cm^{-1} are assigned to C-H stretching vibration.

The bands at 796, 743 and 696cm^{-1} are assigned to C-H in-plane bending modes and the bands at 570, 564, 532 and 508cm^{-1} are identified to C-H out-of-plane bending vibrations. These wave members are in line with the similar compound of 3-Bromo Phenol [14].

3.2.3. Ring vibration

Most of the vibrational bands are affected by the substituents in the aromatic ring. All the carbon atoms within the ring undergo coupled vibrations, called skeletal modes of vibration and exhibit in the region 1660-1420cm^{-1} [28]. In the present investigation, the bands for C-C stretching vibration are appeared at 1699, 1607, 1536, 1487, 1316 & 1292cm^{-1} in FT-IR and 1613, 1321 & 1297cm^{-1} in FT-Raman spectrum. These assignments coincide very well with the earlier reports. Due to O-H substitution in the benzene ring leads to higher C-C stretching vibrations for the phenol compounds.

3.2.4. C-F and C-Cl vibrations

In the vibrational spectra of related molecules, the C-F stretching band which appeared over a wide range of frequency in the region 1360-1000cm^{-1}, is due to the influence of the adjacent substituents. For mono fluorinated compounds the C-F stretching modes appeared in the region 1110-1000cm^{-1}In the present compound 2C5FP, the strong band assigned at 1205cm^{-1} in FT-IR spectrum due to C-F stretching mode. In analogy to these wave members, C-F stretching frequency appeared at 1235cm^{-1} for 1-fluoro-2, 4-dinitrobenzene [29] and M. Karaback *et. al* [30] identified the strong modes at 1254 and 1222cm^{-1} in the FT-IR spectrum. The band at 610cm^{-1} in FT-IR is assigned to C-F in-plane bending mode of vibration. The out-of-plane bending vibration is identified at 244cm^{-1} in FT-Raman spectrum. These wave numbers are supported in the literature data [24, 31].

Generally the C-Cl stretching bands give strong bands in the region 760-505cm^{-1}. The C-Cl stretching mode of the title molecule is found at 729cm^{-1} in the FT-IR spectrum. The in-plane and out-of-plane bending

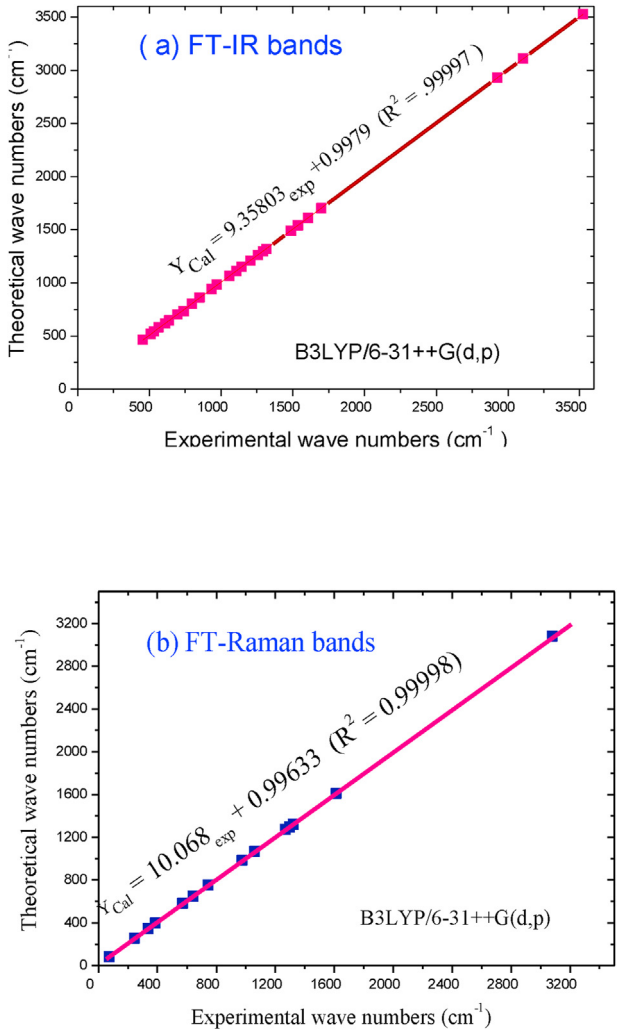

Figure 5. Correlation graphic between the experimental and theoretical IR and Raman wave numbers of 2- chloro-5-fluoro phenol.

assignments C-Cl are identified and presented in Table 2. These vibrational assignments correlate well with the similar compounds of 2, 3, 4, 5-tetrachloro phenol [22].

The correlation between the observed and calculated frequencies is plotted and the corresponding graphics are given in Figure 5. The linear relationship is obtained between the experimental and theoretical wave numbers for IR and Raman, respectively by the following equations:

$$\nu_{Cal} = 0.9979_{Exp} + 9.358\ (R^2 = 0.99997)\ \text{For Infrared} \quad (3)$$

$$\nu_{Cal} = 0.99633_{Exp} + 10.068\ (R^2 = 0.99997)\ \text{For Raman} \quad (4)$$

As a result, the performance of B3LYP/6–31++G (d,p) method with respect to the determination of the wave numbers within the title compound for IR and Raman are quite close.

3.3. Error analysis of different fundamentals

It is a well known fact that the correlation between the observed wave numbers and theoretical wave numbers implies that the systematic errors are due to the regulation in inharmonic effects, lack of basis sets and

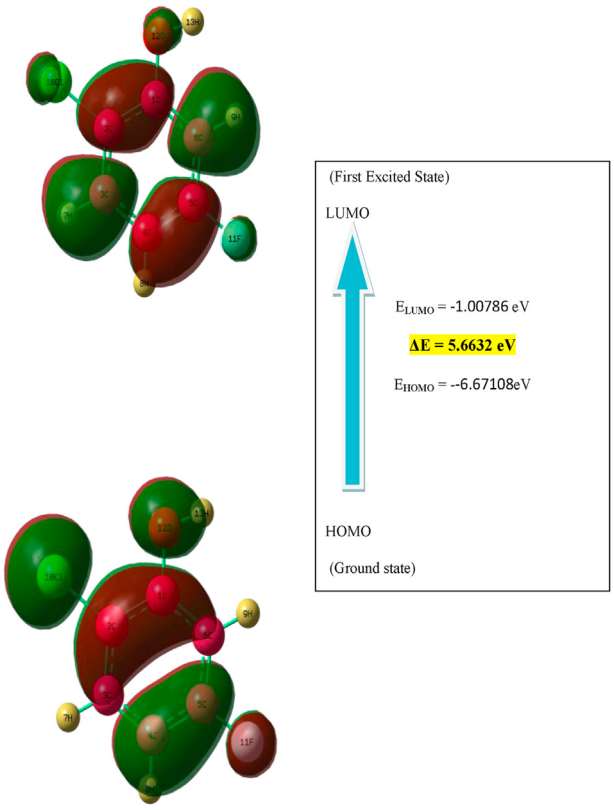

Figure 6. The frontier molecular orbitals of 2- chloro-5-fluoro phenol.

electronic correlations. It is manifest and obvious that the evaluation of standard deviation (S.D) and scale factors provide fine agreement between the experimental and the calculated fundamental modes of vibrations. The RMS deviation and correlation coefficient for observed and calculated wave numbers at B3LYP/6–31++G (d,p) level have been carried out using the following equation [32, 33].

$$RMS = \sqrt{\frac{1}{n-1}\sum_{i}^{n}\left(\nu_i^{calc} - \nu_i^{exp}\right)^2} \quad (5)$$

Where 'n' is the number of observed and calculated data. The RMS error of the frequencies between the unscaled and experimental wave numbers in IR and Raman is found to be 104.567 cm^{-1} and for scaled frequencies it is 8.1557cm^{-1}. In order to refine the observed fundamentals the scale factors were applied between the observed and calculated wave numbers and found to be 0.9858. The correlation graphics between the experimental and calculated wave numbers are quite close to the scaled frequencies as shown in Figure 5.

3.4. Electronic properties

In order to explore the molecular stability and reactivity, the energy gap of HOMO-LUMO is predicted. The key parameters of quantum chemistry is the highest occupied molecular orbital (HOMO) and lowest unoccupied molecular orbital (LUMO). HOMO energy exemplifies the donating electron while LUMO energy symbolizes the accepting electron ability. The energy gap is a crucial parameter for determining the electrical conductivity and other molecular properties of chemical systems

Table 3. Molecular Energy parameters of 2-Chloro-5- fluoro phenol at B3LYP/6–31++G (d,p) method.

Molecular Properties (ev)	Homo Energy	Lumo Energy	Energy gap (ΔE)	Ionisation Potential (I)	Electron Affinity (A)
	-6.67108	-1.00786	5.6632	6.67108	1.00786

Table 4. Global Chemical Parameters of 2-Chloro-5-fluoro phenol at B3LYP/6–31++G (d,p)method.

Molecular Properties (ev)	Electro Negativity	Chemical Potential	Hardness	Softness	Electrophilicity
	χ	μ	η	S	ω
	3.8395	-3.8395	2.832	0.3532	2.603

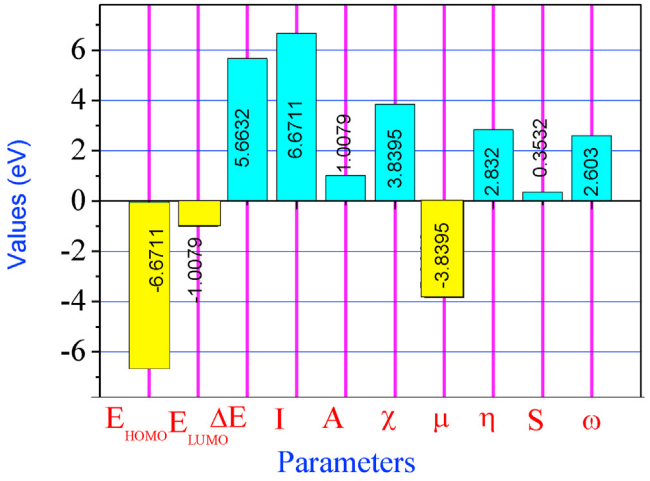

Figure 7. Loaded plot for the Energy parameters (HOMO-LUMO) and global chemical descriptors of 2- chloro-5-fluoro phenol.

and it is also used for predicting the most reactive sites in π-electron systems of molecular species [34, 35]. The theoretically predicted energy gap between HOMO and LUMO for the title compound is found to be 5.6632 eV which reveals that the title compound has a stable structure. The energy difference between the HOMO and LUMO elucidates the eventual charge transfer interaction within the molecular species which influences the NLO activity of the compound. The molecular energy parameter values are given in Table 3. The frontier molecular orbitals of 2C5FP is shown in Figure 6.

3.4.1. Global chemical descriptors

Various reactivity indices have been elucidated within the frame work of density functional theory (DFT). However the electron density is an efficient tool for understanding the chemical reactivity of molecular systems which is based on the electrostatic interactions. The global chemical descriptors such as chemical potential (μ), hardness (η), softness (S) electro negativity (χ) and electrophilicity index (ω) can be determined using HOMO-LUMO energy values for a title molecule at the level of computation B3LYP/6–31++G (d,p) and is incorporated in Table 4. The electronic chemical potential is defined as the escaping tendency of electron from a stable system which can be described as $\mu = -(I + A)/2$. The ionization energy and electron affinity can be derived from HOMO and LUMO orbital energies as $I = -E_{HOMO}$ and $A = -E_{LUMO}$. The mulliken electro negativity is defined as the negative of the chemical potential ($\mu = -\chi$). The hardness is well correlated with the stability and the reactivity of the chemical compound. The chemical hardness which demonstrates the resistance to change in electron distribution is given by $\eta = (I-A)/2$. The inverse of hardness is described as the global softness $S = (1/2\eta)$. Parr *et. al* introduced the concept of the global electrophilicity index (ω) and is calculated using chemical potential and hardness as $\omega = \mu^2/2\eta$. Hardness (η) and softness (S) signify the chemical behavior of the molecular system [36]. Theoretically obtained ionization energy (I), electron affinity (A) and global chemical descriptors of a title molecule are presented in Table 4 and the molecular energy parameter values are depicted in Figure 6.

A soft molecule has a small energy gap and a hard molecule has a large energy gap. It is found that the title molecule 2C5FP has the highest hardness value (η = 2.283 eV) confirms that it is the hardest molecule which means less reactive. A good, more reactive, electrophile is characterized by a higher value of electrophilicity index (ω), while a lower value of ω indicates the presence of a good nucleophile. Hence, the results of the present compound indicate that the title molecule has a lower value of ω (2.603 eV) which proves that is the good nucleophile [37, 38]. The graphical representations of molecular energy parameters and global chemical descriptors are shown in Figure 7.

3.5. Non-linear optical activity

The current research work on the second order non-linear optical (NLO) molecule based on organic materials has been embarked upon due to their potential applications in the field of optoelectronics (such as optical switching and dynamic usage processing) and information technology. Organic materials display a remarkable non-linear optical properties is due to their high molecular hyperpolarizabilites. The first hyperpolarizability of donor acceptor aromatic molecules depends on the electronic charge communication between donor and acceptor groups that is useful in determining the intra- molecular charge transfer. Recently, vibrational spectroscopic determinations combined with quantum chemical calculations have been used as an efficient tool for the investigation of the structural characteristics responsible for the nonlinear optical properties of the molecular systems [39].

Theoretical evaluation of hyperpolarizability is most significant and aids in understanding the relationship between the molecular structure and nonlinear optical properties and is also useful as guideline to experimentalists for the design and synthesis of organic NLO materials. Anju Linda *et. al* studied the theoretical determination of NLO on naphthalene derivatives of p-nitroaniline by using DFT studies. The molecule N-[Naphthalene-5-ly]-4- nitrobenzamine exhibits large hyperpolarizability and hence it can be recommended for photo voltaic device fabrication [40]. In the present investigation, the electronic dipole moment, molecular polarazability, first hyperpolarizability and second order hyperpolarizability are determined using the x, y, z components as follows. According to Kleinmann symmetry, first hyperpolarizability is a third rank tensor that can be described by a 3*3*3 matrix and the 27 components of the 3D matrix can be deduced to 10 components.

The complete equations for evaluating the magnitude of dipole moment (μ), polarizability(α), first hyperpolarizability (β) and second hyperpolarizability (γ) using the x,y,z component are as follows [41].

$$\text{Dipole moment } \mu = \left(\mu_x^2 + \mu_y^2 + \mu_z^2\right)^{\frac{1}{2}} \quad (6)$$

$$\text{Polarizability } \alpha = \frac{\alpha_{xx} + \alpha_{yy} + \alpha_{zz}}{3} \quad (7)$$

$$\text{First hyperpolarizability } \beta = \left(\beta_x^2 + \beta_y^2 + \beta_z^2\right)^{\frac{1}{2}} \quad (8)$$

Here

Table 5. Calculated Non Linear Parameters of 2-Chloro-5-fluoro phenol at B3LYP/6–31++G (d,p) method.

Non Linear Parameters	Dipole Moment (μ/D)	Polarizability (α)	First Hyper Polarizability (β)	Second Order hyperPolarizability (γ)
	1.4083 Debye	10.1768×10^{-24}esu	2.0953×10^{-30}esu	-2927.24×10^{-40}esu

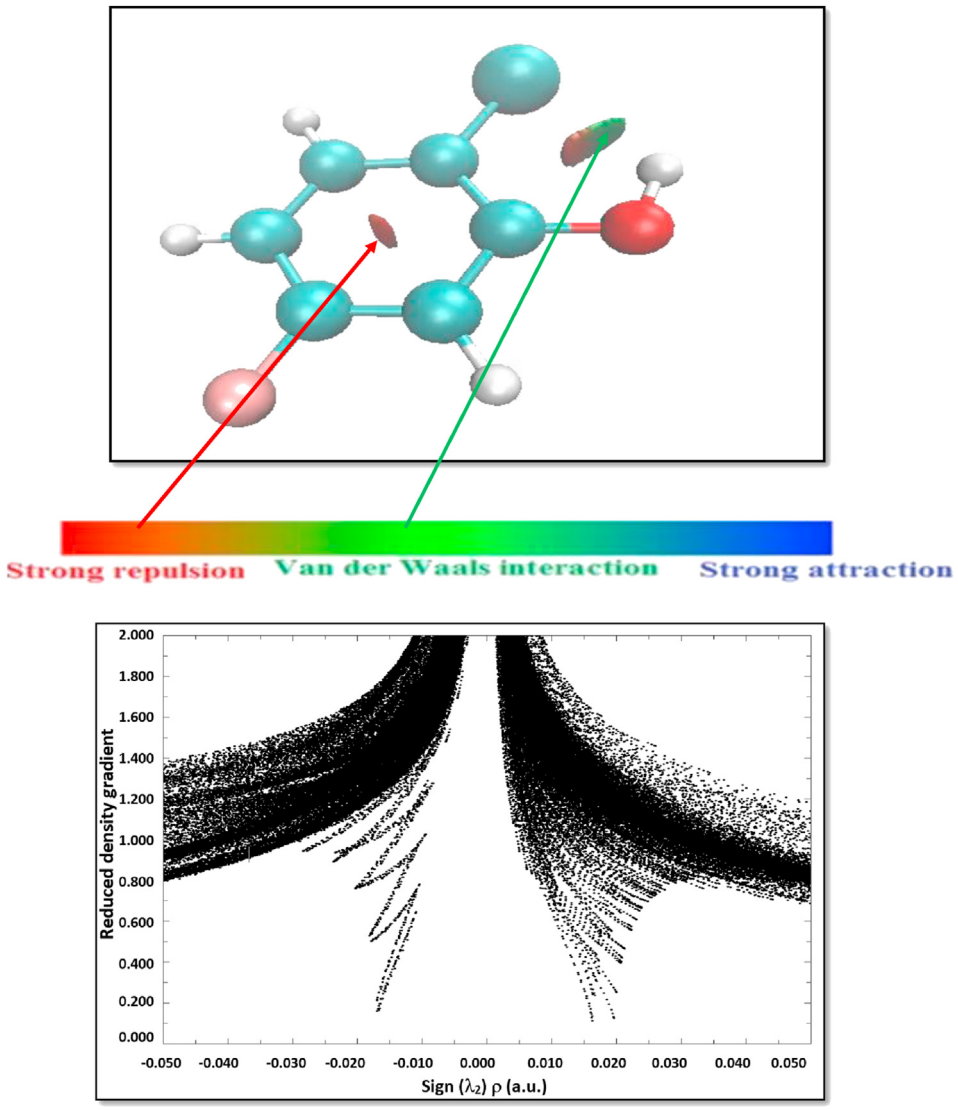

Figure 8. The Reduced density gradient of 2-chloro-5-fluoro phenol molecule according to λ_2.

$$\beta_x = \beta_{xxx} + \beta_{xyy} + \beta_{xzz}$$
$$\beta_y = \beta_{yyy} + \beta_{xxy} + \beta_{yzz}$$
$$\beta_x = \beta_{zzz} + \beta_{xzz} + \beta_{yyz}$$

$$\text{Second order hyperpolarizability } \gamma = \frac{\left[\gamma_{xxxx} + \gamma_{yyyy} + \gamma_{zzzz} + 2\left(\gamma_{xxyy} + \gamma_{xxzz} + \gamma_{yyzz}\right)\right]}{5} \tag{9}$$

The Non – Linear optical (NLO) parameters of the title molecule have been computed by using B3LYP with 6-31+G (d,p) level and the corresponding values are given in Table 5. Since the values of the non linear optical parameters of Gaussian output are in atomic units (a.u) the calculated values are converted into electrostatic units (esu) (α: 1a.u = $0.1482*10^{-24}$ esu, β: 1 a.u = $0.86399*10^{-32}$ esu, γ: 1 a.u = $5.0372*10^{-40}$ esu) [42]. The calculated first hyperpolarizability of the present molecule (β = $2.0953*10^{-30}$ esu) is about 7 times greater than urea (β = $0.28166*10^{-30}$ esu). The reported value of first hyperpolarizabiliy of similar structure is β = $2.8065*10^{-30}$ esu [43].

Hence, from the results of the present molecule 2C5FP refined that it supports in the development of new effective material for NLO applications.

3.6. Reduced density gradient (RDG)

RDG analysis is used to evaluate the weak interaction based on electron density as a dimensionless quantity developed by Johnson *et. al* [44] and its first gradient is given by

$$RDG = (r) = \frac{1}{2(3\pi r^2)^{1/3}} \frac{|\Delta^2 \rho(r)|}{\rho(r)^{4/3}} \tag{10}$$

By analyzing the low density gradient values and the high density gradient values can be identify the weak and strong interactions. The plot of ρ(r) Vs λ_2 describes the nature and strength of interaction. The sign λ_2 which is the highest value of Lessian matrix of electron density helps to identify the nature of interaction by color code. The RDG analysis was performed by using multiwfn software [20] followed by VMD programme. The predicted RDG plot for the title molecule (2C5FP) is shown in Figure 8. In the present molecule (2C5FP), the blue color represents the strong hydrogen bond interaction, red and green colors represent the strong repulsion and Van der Waals (VDW) interaction, respectively. These interactions can be responsible for the stability of the molecular system.

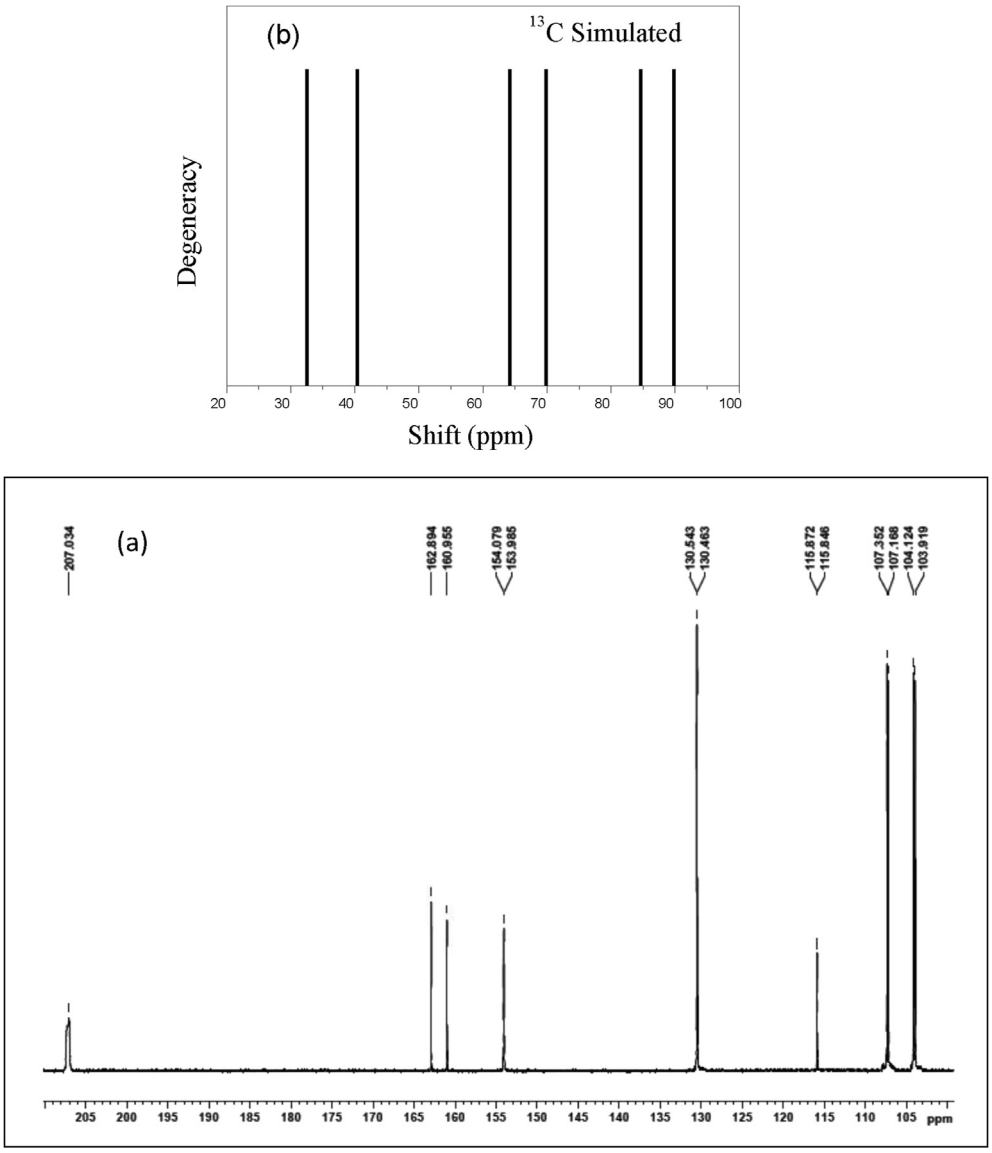

Figure 9. (a) Experimental and (b) Calculated (B3LYP/6–31++G (d,p)) ^{13}C NMR spectrum of 2 chloro-5-fluoro phenol.

3.7. NMR chemical shifts

A combined NMR spectroscopic analysis and computer simulation technique offer a unique way to intercept and predict the chemical structure of large biomolecules. For instance, ^{13}C chemical shift is one of the most pioneer techniques in determining the presence and absence of specific atom in a specific position of a molecular system [45]. Chemical shifts of 2C5FP are performed using the Gauge invariant atomic orbital (GIAO) method at 6–31++G (d,p) level in the gaseous phase. The GIAO method is one of the most significant and common approaches for evaluating isotropic nuclear magnetic shielding tensors. The obtained theoretical and experimental ^{1}HNMR and ^{13}CNMR spectra of 2C5FP are shown in Figures 9 and 10, respectively. The experimental ^{1}HNMR and ^{13}CNMR were recorded using acetone solvent and their corresponding chemical shifts (δ) for protons and carbon atoms were observed. The isotropic chemical shifts δ can be evaluated using isotropic shielding data with respect to Tetramethylsilane (TMS) [42]. The relationship between the chemical shift (δ) and isotropic shielding (σ) for carbon atom is given by

$$\delta_{iso}(C) = \sigma_{TMS}(C) - \sigma_{iso}(C) \quad (11)$$

Where δ_{iso} is the isotropic chemical shift, σ_{iso} is the isotropic shielding and C is the carbon atom [46]. The isotropic shielding value of carbon atoms and hydrogen atom in Tetramethylsilane (TMS) at B3LYP/6–31++G (d,p) level of computation is found to be 195.272ppm and 32.362 ppm, respectively. The experimental and calculated chemical shifts data with respect to TMS of 2C5FP in gas phase and acetone, chloroform solvents are shown in Table 6.

Generally, the CNMR isotropic chemical shifts of organic molecules are lying in the region 10–200 ppm. In the aromatic molecule, the carbon (^{13}C) and proton (^{1}H) chemical shifts are observed in the range of 115–150 ppm and 7.00–8.00 ppm. In the present investigation, theoretical ^{13}CNMR spectrum makes out that the largest deshielded signal of the C5 and C1 atom is found to be 162.74 (gas), 163.24(acetone), 163.10 ppm (chloroform) and 154.91 (gas), 154.63 ppm (chloroform) 154.51 ppm (acetone), respectively. These can be attributed to the bond formed with electro negative atoms. Such electro negative atom polarizes the charge distribution in its bond to the adjacent carbon atom and reduces the electron density at the bridge for the title molecule. In the present compound, the carbon atoms C1 and C5 attached to the oxygen and fluorine atoms, respectively. Particularly, the ^{13}C chemical shifts of atom C5 are

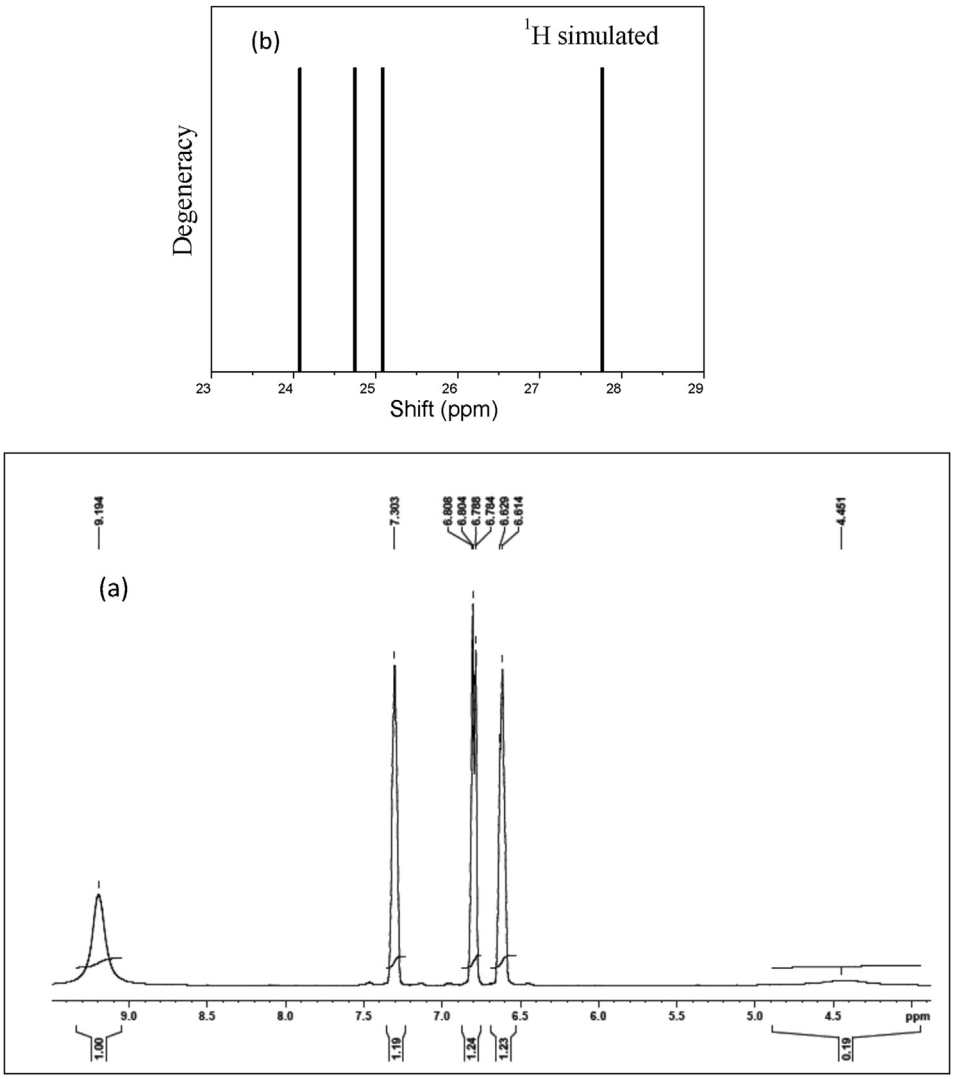

Figure 10. (a) Experimental and (b) Calculated (B3LYP/6–31++G (d,p)) ^{1}H NMR spectrum of 2- chloro-5-fluoro phenol.

Table 6. Experimental and Theoretical ^{13}C and ^{1}H isotropic chemical shifts (with respect to TMS) for 2- Chloro- 5-fluoro phenol at B3LYP/6–31++G (d,p) method.

Atom / Values in ppm	Exp Acetone	Acetone	Chloroform	Gas phase
C1	154.52	154.51	154.63	154.91
C2	123.76	123.75	124.20	125.41
C3	131.01	130.97	131.02	131.07
C4	112.53	111.45	111.22	110.65
C5	163.29	163.24	163.10	162.74
C6	106.83	106.87	106.45	105.46
H7	8.52	8.47	8.42	8.29
H8	7.82	7.84	7.78	7.62
H9	7.75	7.71	7.59	7.28
H13	5.42	5.41	5.21	4.60

slightly over estimated than C1, because the electro negativity of fluorine atom is greater than the oxygen. The ^{13}C NMR chemical shifts were experimentally recorded in acetone at the interval of 112.53–163.29 ppm, which extensively coherence with the theoretically performed ^{13}CNMR chemical shifts in acetone. The DFT showed a smaller change in carbon and proton chemical shifts with solvent than the experimentally observed data. The experimental proton (^{1}H) chemical shifts of 2C5FP was recorded in the range of 5.42–8.52ppm. The correlated computational chemical shifts of proton in acetone are 8.29,7.62,7.28 and 4.60ppm. Proton next to electron-donating groups are shielded likewise electron-withdrawing groups are deshielded [47]. Due to this, proton numbered H7 (8.29),H8 (7.62) and H9 (7.28) ppm have the maximum chemical shift values, as it is near the electro negative atoms such as 10Cl,11F and O12. These results

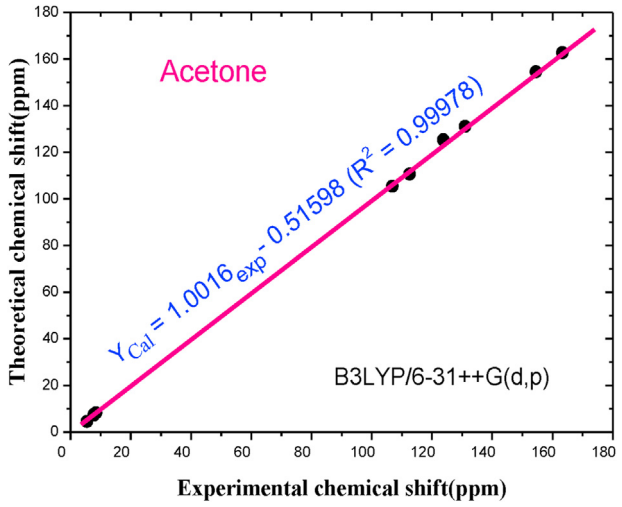

Figure 11. Correlation graphic between the experimental and theoretical chemical shifts of 2- chloro- 5- fluoro phenol.

concede that the experimental and theoretical chemical shifts are well consistent with each other.

The linear relation between the experimental ^{13}C and ^{1}H chemical shifts and the gauge – including atomic orbital (GIAO) magnetic isotropic shielding tensors is described by the following equation

$$\delta_{exp} = a+b\sigma_{cal} \quad (12)$$

Where, the intercept (a) and slope (b) of the least squares correlation line is used to scale the theoretical (GIAO)/B3LYP/6-31+G (d,p) isotropic shielding tensors σ and to predict the chemical shifts. The correlation graphics between the experimentally and calculated chemical shifts of the title molecule is depicted in Figure 11. The linear equations obtained between the experimental and calculated chemical shifts are described as

$$\delta_{Cal} = 10016_{Exp} - 0.51598\ (R^2 = 0.9998)\ \text{Acetone} \quad (13)$$

3.8. Hydrogen bond and thermodynamic properties

Hydrogen bond is extremely powerful in deriving information such as weak molecular interactions, molecular conformations and dynamics in

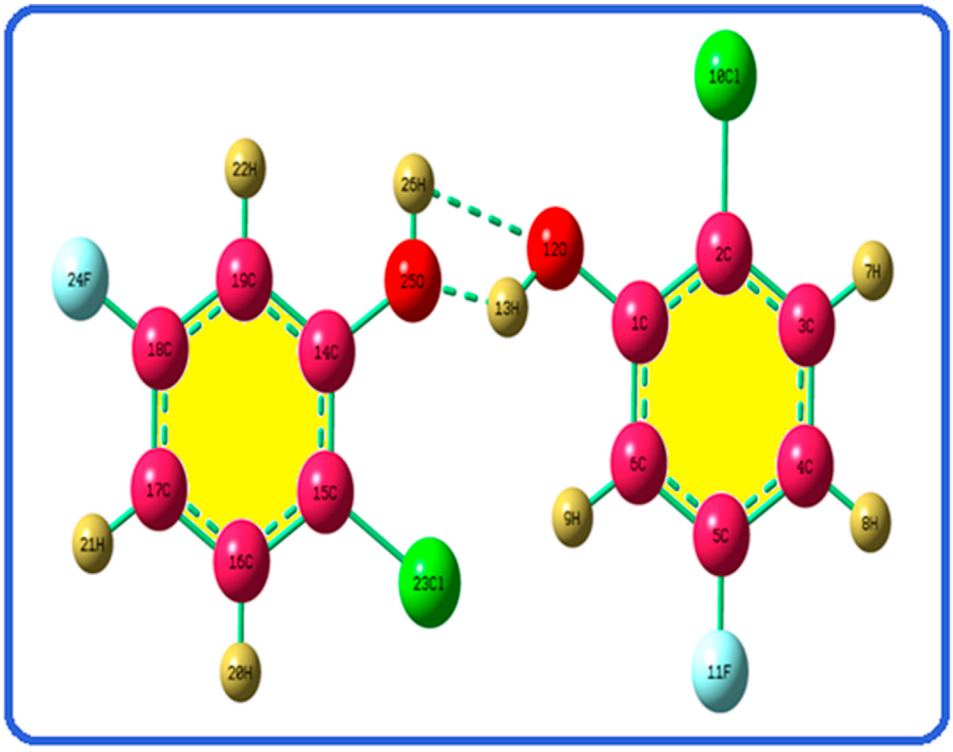

Figure 12. Dimer structure of 2-chloro-5-fluoro phenol.

Table 7. Calculated thermodynamic functions of 2-Chloro- 5-fluoro phenol using B3LYP/6–31++G (d,p) method.

Temperature	Thermodynamic parameters		
	C_p	S_m	H_m
(K)	(cal $mol^{-1}k^{-1}$)	(cal $mol^{-1}k^{-1}$)	(k cal mol^{-1})
100	10.975	63.888	55.184
200	20.363	75.77	56.754
300	28.903	86.465	59.227
400	36.16	96.399	62.492
500	41.987	105.563	66.411
600	46.547	114.001	70.847
700	50.13	121.762	75.687

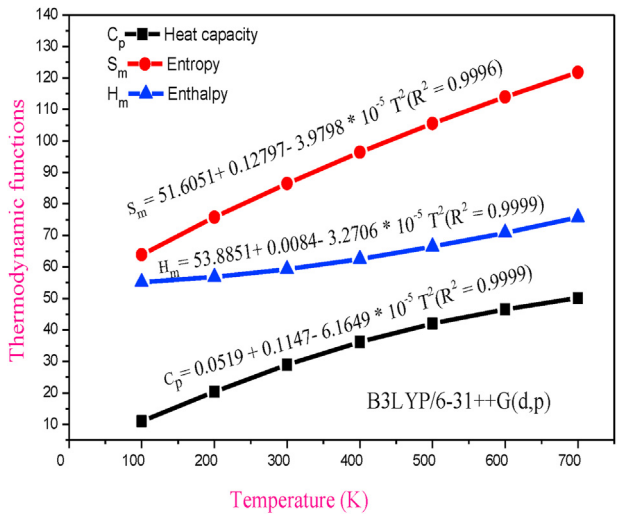

Figure 13. Variation of thermodynamic functions with temperature of 2-chloro-5-fluoro phenol.

the solid state. Intra and inter-molecular interactions play a pivotal role in many disciplines such as host-guest chemistry, organic chemistry, pharmacology, biochemistry and molecular biology. For instance, the key factor is the breakage or dissociation of intramolecular and intermolecular hydrogen bond in the dissolution of cellulose [48, 49]. In the present investigation, the existence of intra and inter molecular hydrogen bonding is interpreted through the analysis of structural parameters. The dimer structure of the title molecule is shown in Figure 12. The intermolecular hydrogen bonded distances 12O … 26H = 1.99A^{0}and25O … 13H = 1.99A^0 are lesser than the sum of van der Walls radii (2.7 Å for O … H) which strongly validates the presence of intermolecular H- bridge bonds [28].

3.8.1. Thermodynamic properties

On the basis of vibrational evaluation the standard statistical thermodynamic parameters such as heat capacity, entropy and enthalpy are computed using B3LYP/6–31++G (d,p) basis set. The total energy of a molecular system is the sum of translational, rotational, vibrational and electronic energies ie $E = E_t + E_r + E_v + E_{e..}$ Thermodynamic quantities such as heat capacity at constant pressure (C_p), entropy (S_m) and enthalpy (H_m) for various ranges of temperature (100–700) are evaluated and the corresponding values are presented in Table 7. It can be noticed that the thermodynamic quantities increased with the increase of temperature from 100 to 700k. All thermodynamic computations have been carried out in gas phase. The correlation equations of heat capacity (C_p), entropy (S_m), and enthalpy (H_m) change to temperatures that are fitted by parabolic formula and the corresponding fitting factors (R^2) for these thermodynamic functions are found to be 0.9999, 0.9996 and 0.9999, respectively. The corresponding fitting equations of 2C5FP are as follows and the correlation graphics are depicted in Figure 13.

$$C_P = 0.0519 + 0.1147–6.6149 *10^{-5} T^2 (R^2 = 0.9999) \quad (14)$$

$$S_m = 51.605 + 0.12797–3.9798 *10^{-5} T^2 (R^2 = 0.9996) \quad (15)$$

$$H_m = 53.885 + 0.004–3.2706 *10^{-5} T^2 (R^2 = 0.9999) \quad (16)$$

Hence, all these thermodynamic properties provide useful information for future study on 2C5FP [41, 50].

3.9. In – vitro antibacterial determination assay

3.9.1. Test bacterial samples

The selected bacterial strains were used for the title compound viz., *Streptococcus aureus, Staphylococuss aureus,* (Gram – positive bacteria), *Escherichia coli* and *Pseudomonas aureus* (Gram – negative bacteria), respectively. The bacterial strains were cultivated in Muller – Hinton agar plates and then inoculated plates were incubated at 37^{0}c for24h for antibacterial sensitivity assay.

3.9.2. Interpretation of antibacterial activity

The antibacterial activity of the title molecule 2C5FP is performed by the disc diffusion method. The most influencing factor exhibits significant antibacterial effect in phenol compounds which is due to the presence of rich plant extracts in phenolic compounds and the other factors are molecular weight, chemical reactivity, hydroxy group and electro negativity of atoms in the compound. The substitution of the electron-donating –OH moiety and electron-withdrawing groups such as fluorine (F) and oxygen (O) on the benzene ring of the title compound are the most significant that contributes to the antibacterial activity [51]. The presence of high electronegative atoms such as oxygen and fluorine atoms which are larger values of the negative charges on the molecule 2C5FP suggest the high electron density of the centers that would preferentially interact with micro-organisms then increases the antibacterial potential. On the other hand, the presence of the proton exchangeability of the phenolic –OH, attached to the electron delocalized system with high proton binding affinity contributes to the ability of penetration and damaging the cytoplasmic membranes, thus enhancing the antibacterial activity [52].

The HOMO-LUMO energy gap is the most significant tool for the chemical reactivity as well as the biological activity of the molecules. The presence of energy gap promotes the detachment of one electron from the molecule and can migrate inside the micro-organism producing free radicals that can damage and contribute to kill the pathogens. The distribution of the electron density or electrostatic potential surface area is an important factor to identify the electrophilic and nucleophilic site over the molecule and the charged surface area in a compound that is considered as the best parameter to estimate the biological activity. According to the mechanism of the antibacterial activity of the compounds, the positive charge on the end of the molecules is responsible for the damage to the plasma membrane of pathogenic micro-organisms. In the present compound, the higher positive charged regions of oxygen and fluorine atoms are involved in the biologically active part in the molecule as well as used to inhibit the pathogens [53].

The observed data of antibacterial activity of the title molecule (2C5FP) and the standard drug are shown in Table 8 and the corresponding diagram depicted in Figures 14 and 15. From the results, it is

Table 8. The Antibacterial activity of 2- Chloro- 5-fluoro phenol at different concentrations against bacterial pathogens.

S.NO	Cultures	Diameter of the Zone of Inhibition in mm					
		10µl	20µl	30µl	40µl	Control	Antibiotic
1	*Escherichia coli*	-	-	8	12	Nil	17
2	*Staphylococcus aureus*	-	8	10	12	Nil	16
3	*Pseudomonas aureus*	-	-	8	12	Nil	16
4	*Streptococcus aureus*	-	8	12	13	Nil	Nil

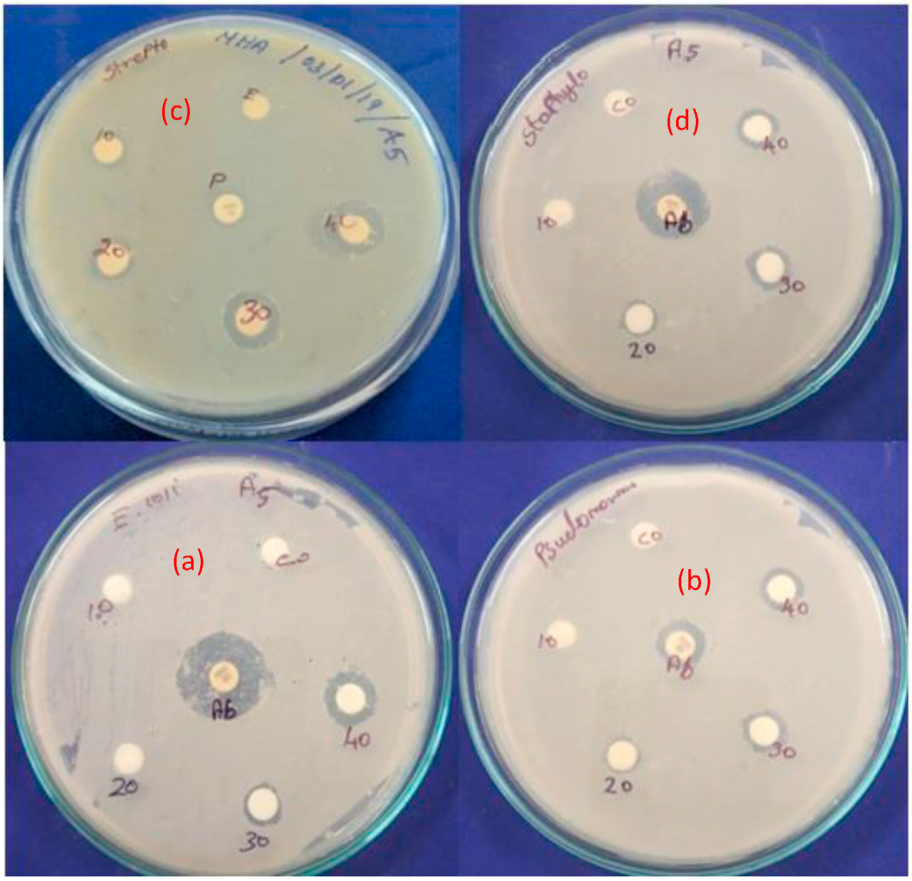

Figure 14. Disk diffusion method of 2-chloro-5-fluoro phenol at different concentrations; (a) *Escherichia coli* (b) *Pseudomonas aureus* (c) *Streptococcus aureus*; (d) *Staphylococcus aureus*.

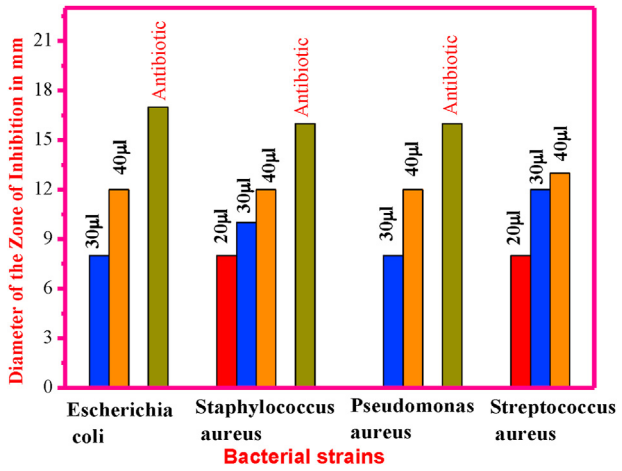

Figure 15. A bar diagram plot for the antibacterial activity of 2-chloro-5-fluoro phenol.

observed that the title compound is recognized to be the potential antibacterial scaffold with the average zone of inhibition 8–13 mm against bacterial strains. The title compound is compared with Amoxicillin as standard antibiotic. The title molecule 2C5FP exhibits good antibacterial activity against Gram-positive bacteria such as *Streptococcus aureus, Staphylococcus aureus* and exhibits low activity against Gram- negative bacteria such as *Escherichia coli* and *Pseudomonas aureus.* Particularly, the molecule 2C5FP exhibits very effective activity in higher concentration (40µL) for all selected pathogens. Among the selected bacterial strains, the title compound (2C5FP) exhibits better activity against *streptococcus aureus* when compared to standard antibiotic. The tested compound exhibits better activity against the Gram-Positive bacteria rather than Gram-negative bacterial strains.

3.9.3. Molecular docking analysis

The molecular docking technique is used recently in the biological study for drug discovery and to get insight in to the exact binding location of the protein and ligands. It predicts the interaction between two molecules with overall minimum energy and the best orientation of protein-ligand [54]. The molecular docking analysis was performed on the most active compound 2C5FP against *staphylococcus aureus* tyrosyl-tRNA

Table 9. Molecular docking results of 2-Chloro-5-fluoro phenol molecule with 1JIL and 6CJF protein targets.

Drug	Protein (PDB ID)	Binding Energy (kcal/mol)	RMSD (A^0)	No. of Hydrogen Bond	Bonded Residues	Bond Distance (A^0)
2C5FP	1JIL	-3.80	112.20	2	Protein: A: ASN 29	1.7
					Protein A: ASN 3	2.3
	6CJF	-4.33	29.74	2	Protein A: THR 63	2.8
					Protein A: GLY 66	2.1

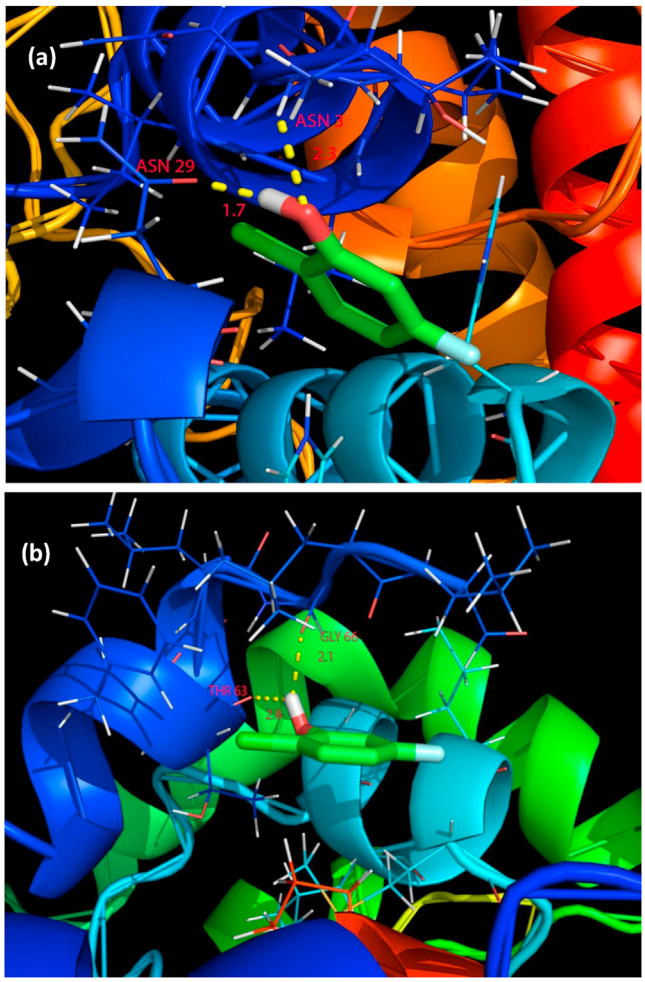

Figure 16. Docking and hydrogen bond interaction of ligand 2-chloro-5- fluoro phenol with two proteins (a) 1JIL (b) 6CJF.

synthetase (PDB ID: 1JIL) and hDHODH inhibitor (PDB ID: 6CJF). The results of antibacterial screening reveal that the title compound 2C5FP displayed good inhibitory activity against *staphylococcus aureus* as compared to the standard drug. The suitable target protein 6CJF (PDB: ID) is a flavin-dependent mitochondrial enzyme of Dihydroorotate Dehydrogenase (hDHODH) protein. Such enzyme has been associated with autoimmune diseases as well as cancers. In current research, hDHODH inhibitors have been proved as an effective drug against rheumatoid arthritis, multiple sclerosis, inflammatory disorders and cancer therapy as studied by Ahmed. F. Abdel-Magnd [55, 56, 57]. The molecular docking is performed on 2C5FP as a ligand with the selected proteins using Auto dock Vina software. The title molecule 2C5FP (ligand) is selected to be the active site of the proteins and the minimum energy value is obtained. The molecular docking lowest binding energies (kcal/mol), RMSD (A^0) and bond distance (A^0) along with the residues are listed in Table 9. According to obtained docking results, it is conceded that the docked ligand 2C5FP form a stable complex with the receptors (Figure 16). In Figure 16, yellow dotted line represents the formation of intermolecular hydrogen bond between the ligand 2C5FP and with two different proteins [58].

Hydrogen bonds are another significant factor that influences protein stability and contributes to the stability of proton-ligand binding interactions. An intermolecular hydrogen bond is formed with donor atom (D) and a hydrogen atom (H) in one compound and an acceptor atom (A) in the other compound. The donor group in a hydrogen bond is a strongly electronegative atom such as O, N and F that is covalently bonded to a hydrogen bond. The hydrogen acceptor is an electronegative atom of a neighboring compound that contains a lone pair that involves in the hydrogen bond [59]. The docking computation confirms that the O-H moiety is engaged in hydrogen bonding with the amino acids and shows π-anion interaction with benzene ring. The docking computed results confirm that ASN 29 and ASN 3 amino acids form hydrogen bond interaction with a bond length of 1.7 A^0 and 2.3 A^0, respectively, for 1JIL protein. Likewise, GLY 66 and THR 63 amino acids form a hydrogen bond interaction with a bond distance of 2.1 A^0 and 2.8 A^0, respectively, for 6CJF protein. These hydrogen bonds play a positive role in strengthening the binding effect between the ligand and protein [60]. In consequence, the molecular docking analysis demonstrated an enhancement of the ligand that has good pharmacological properties with the proteins.

4. Conclusion

The title molecule 2C5FP was characterized by various spectroscopic techniques (FT-IR, Raman and NMR). The optimized structural parameters such as bond lengths and bond angles of monomer and dimer of the title molecule compared with X – ray crystallographic data of related compound is found to have reliable agreement. The complete vibrational analysis has been performed and it is conceded that the relation between experimental and calculated wave numbers is found to be quite close. Non linear optical behavior of the title compound has been investigated by the first and second hyper polarazibility. Theoretically predicted ^{13}C and ^{1} H NMR chemical shifts of title molecule is compared with experimental data in acetone solvent enhances a very good agreement. The correlations between the statistical thermodynamics and temperature are obtained and discussed. The charge transfer mechanism is attained with in a molecule by determining the energy gap between HOMO and LUMO and reactivity parameters. The title molecule 2C5FP exhibited better antibacterial activity against Gram-positive bacteria rather than Gram-negative bacterial strains. Finally, from the molecular docking results, the low binding energy of -3.8kcal/mol confirm that the title compound 2C5FP is a good antibacterial compound.

Declarations

Author contribution statement

M. Arivazhagan: Conceived and designed the experiments; Contributed reagents, materials, analysis tools or data.

V. Vidhya: Analyzed and interpreted the data; Wrote the paper.

A. Austine: Conceived and designed the experiments; Performed the experiments.

Funding statement

This research did not receive any specific grant from funding agencies in the public, commercial, or not-for-profit sectors.

Declaration of interests statement

The authors declare no conflict of interest.

Additional information

No additional information is available for this paper.

Acknowledgements

The authors are grateful to the Indian Institute of Technology (IIT), Chennai, India for experimental study and Dr. P. Kavitha, Head, Associate Professor, Dr. C. Thiyagarajan, Assistant Professor, Department of Microbiology, Srimad Andavan College, Trichy, India and Dr. S. Sebastian, Department of Physics, St. Joseph's College of Arts & Science, Cuddalore Tamilnadu, India for the biological studies.

References

[1] Ashley G. Muller, Satyajit D. Sarker, Imran Y. Saleem, Gillian A. Hutcheon, Delivery of natural phenolic compounds for the potential treatment of lung cancer, DARU J. Pharm. Sci. 27 (2019) 433–449.

[2] Ioana Ignat, Irina Volf, Valentin I. Popa, A critical review of methods for characterisation of polyphenolic compounds in fruits and vegetables,, Food Chem. 126 (2011) 1821–1835.

[3] Prithviraj Karak, Biological activities of flavonoids: an overview, Int. J. Pharma Sci. Res. 10 (2019) 1567–1574.

[4] Shagufta Perveen, Areej Mohammad Al-Taweel, Phenolic Compounds from the Natural Sources and Their Cytotoxicity, INTECH, Kingdom of Saudi Arabia, 2017.

[5] Yeganeh Entezari Heravi, Silvia Bua, Alessio Nocentini, Sonia Del Prete, Ali Akbar Saboury, Hassan Sereshti, Clemente Capasso, Paola Gratteri, Claudiu T. Supuran, Inhibition of Malassezia globosa carbonic anhydrase with phenols, Bioorg. Med. Chem. 25 (2017) 2577–2582.

[6] Yundong Xie, Yaping Yang, Sen Li, Yanhong Xu, Wenfang Lu, Zizhang Chen, Guangde Yang, Yiping Li, Yongxiao Cao, Xiaoli Bian, Phenylsulfonylfuroxan NO-donor phenols: synthesis and multifunctional activities evaluation, Bioorg. Med. Chem. 25 (2017) 4407–4413.

[7] Merve Bacanli, A. Ahmet Başaran, Nurşen Başaran, Cytotoxicity evaluation of some phenolic compounds in V79 cells, Turk. J. Pharm. Sci. 12 (2015) 299–304.

[8] Swapna Upadhyay, Madhulika Dixit, Role of polyphenols and other phytochemicals on molecular signaling, Oxid. Med. Cell. Longev. 2015 (2015) 1–15.

[9] Magdalena Działo, Justyna Mierziak, Urszula Korzun, Marta Preisner, Jan Szopa, Anna Kulma, The potential of plant phenolics in prevention and therapy of skin disorders, Int. J. Mol. Sci. 17 (2016) 1–41.

[10] S. Ramalingam, S. Periandy, M. Karabacak, N. Karthikeyan, Spectroscopic (FT-IR/FT-Raman) and computational (HF/DFT) investigation and HOMO/LUMO/MEP analysis on 2-amino-4-chlorophenol, Spectrochim. Acta 104 (2013) 337–351.

[11] Gui-Xiang Wang, Xue-Dong Gong, Yan Liu, He-Ming Xiao, A theoretical study on the vibrational spectra and thermodynamic properties for the nitro derivatives of phenols, J. Spectrochim. Acta A 74 (2009) 569–574.

[12] V. Balachandran, M. Murugan, V. Karpagam, M. Karnan, G. Ilango, Conformational stability, spectroscopic (FT-IR & FT-Raman), HOMO–LUMO, NBO and thermodynamic function of 4-(trifloromethoxy) phenol, J. Spectrochim. Acta A 130 (2014) 367–374.

[13] N. Sunderaganesan, B. Anand, C. Meganathan, B. Dominic Joshua, FT-IR, FT-Raman spectra and *ab-initio* HF, DFT vibrational analysis of 2,3-difluoro phenol, J. Spectrochim. Acta A 68 (2007) 561–566.

[14] D. Mahadevan, S. Periandy, S. Ramalingam, Vibrational spectroscopy (FT-IR and FT Raman) investigation using *ab-initio* (HF) and DFT (B3LYP) calculations on the structure of 3-Bromo phenol, J. Spectrochim. Acta A 78 (2011) 575–581.

[15] S. Murugavel, N. Manikandan, D. Lakshmanan, Kanagaraj Naveen, Paramasivan Thirumalai Perumal, Synthesis, crystal structure, dft and antibacterial activity studies of (E)-2-Benzyl-3- (Furan-3-Yl)-6,7-Dimethoxy-4-(2-Phenyl-1h-Inden-1-Ylidene)-1,2,3,4-Tetrahydroisoquinoline, J. Chil 60 (2015) 3015–3020.

[16] M. Fathimunnisa, H. Manikandan, K. Neelakandan, N. Rajendra Prasad, S. Selvanayagam, B. Sridhar, Synthesis, characterization, biological evaluation and docking studies of 2′-[(2″,4″-difluorobiphenyl-4-yl)carbonyl]-1′-aryl-1′,2′,5′,6′,7′,7a′-hexahydrospiro[indole-3,3′-pyrrolizin]-2(1H)-ones, J. Mol. Struct. 1122 (2016) 205–218.

[17] M. Fathimunnisa, H. Manikandan, S. Selvanayagam, Synthesis of novel (2E)-1-[4-(2,4-difluorophenyl)phenyl]3-arylprop2-en-1-ones: investigation on spectral, antibacterial, molecular docking and theoretical studies, J. Mol. Struct. 1122 (2016) 205–218.

[18] Mauricio Alcolea Palafox, V.K. Rastogi, Quantum chemical predictions of the vibrational spectra of polyatomic molecules: the uracil molecule and two derivatives, J. Spectrochim. Acta A58 (2011) 411–440.

[19] T. Sundius, Scaling of *ab-initio* force fields by MOLVIB, J. Vib. Spectrosc. 29 (2002) 89–95.

[20] S. Sangeetha Margreat, S. Ramalingam, S. Sebastian, S. Xavier, S. Periandy, Joseph C. Daniel, M. Maria Julie, DFT, spectroscopic, DSC/TGA, electronic, biological and molecular docking investigation of 2,5-thiophenedicarboxylic acid: a promising anticancer agent, J. Mol. Struct. 1200 (2020) 127099–127114.

[21] Warren L. DeLano, PyMOL: an Open-Source Molecular Graphics Tool, Delano Scientific LLC Copyright, 2009. California USA.

[22] C. Bavoux, P. Michel, Structure crystalline dichloro-2,6 phenol, J. Acta. Crysto B and Crys. Chem. 30 (1974) 2043–2045.

[23] Wiktor Zierkiewicz, Danuta Michalska, Thérèse Zeegers-Huyskens, Molecular structures and infrared spectra of p-chlorophenol and p-bromophenol. Theoretical and experimental studies, J. Phys. Chem. 104 (2000) 11685–11692.

[24] Mehmet Karabacak, Etem Kose, Ahmet Atac, M. Ali Cipiloglu, Mustafa Kurt, Molecular structure investigation and spectroscopic studies on 2, 3-difluorophenylboronic acid: a combined experimental and theoretical analysis, J. Spectrochim. Acta A 97 (2012) 892–908.

[25] R. Meenakshi, Experimental (FT-IR and FT-Raman) and spectroscopic investigations, electronic properties and conformational analysis by PES scan on 2-methoxy-5-nitrophenol and 2-methoxy-4-methylphenol, J. RSC Adv. 6 (2016) 1822–1831.

[26] V. Krishnakumar, N. Jayamani, R. Mathammal, K. Parasuraman, Density functional theory calculations and vibrational spectra of 2-bromo-4-chloro phenol and 2-chloro-4-nitro phenol, J. Raman Spectrosc. 40 (2009) 1551–1556.

[27] V. Balachandran, S. Rajeswari, S. Lalitha, Vibrational spectral analysis, computation of thermodynamic functions for various temperatures and NBO analysis of 2,3,4,5-tetrachlorophenol using *ab-initio* HF and DFT calculations, J. Spectrochim. Acta A 101 (2013) 356–369.

[28] M. Arivazhagan, R. Kavitha, Molecular structure, vibrational spectroscopic, NBO, HOMO–LUMO and Mulliken analysis of 4-methyl-3-nitro benzyl chloride, J. Mol. Struct. 1011 (2012) 111–120.

[29] A.K. Ansari, P.K. Verma, Laser Raman and IR. spectra of 1-fluoro 2,4-dinitrobenzene, J. Spectrochim. Acta A 35 (1979) 35–36.

[30] Mehmet Karabacak, Etem Kose, Mustafa Kurt, FT-Raman, FT-IR spectra and DFT calculations on monomeric and dimeric structures of 5-fluoro- and 5-chloro-salicylic acid, J. Raman Spectrosc. 41 (2010) 1085–1097.

[31] N. Sundaraganesan, S. Ilakiamani, B. Dominic Joshua, FT-Raman and FT-IR spectra, ab initio and density functional studies of 2-amino-4,5-difluorobenzoic acid, J. Spectrochim. Acta A 67 (2007) 287–297.

[32] Ozlem Mihciokur, Talat Ozpozan, Molecular structure, vibrational spectroscopic analysis (IR & Raman), HOMO-LUMO and NBO analysis of anti-cancer drug sunitinib using DFT method, J. Mol. Struct. 1149 (2017) 27–41.

[33] V. Vidhya, A. Austine, M. Arivazhagan, Molecular structure, aromaticity, vibrational investigation and dual descriptor for chemical reactivity on 1-chloroisoquinoline using quantum chemical studies, Res. Mater. 6 (2020) 100097, 1–17.

[34] J. Daisy Magdaline, T. Chithabarathanu, Vibrational spectroscopic investigations, conformational study, natural bond orbital and HOMO-LUMO analysis of 2-benzoyl thiophene, Asian J. Chem. 27 (2015) 4600–4610.

[35] S. Sivaprakash, S. Prakash, S. Mohan, Sujin P. Jose, Quantum chemical studies and spectroscopic investigations on 2-amino-3- methyl-5-nitropyridine by density functional theory, Heliyon 5 (2019), e02149, 1–10.

[36] G. Bharathy, Johanan Christian Prasana, S. Muthu, Molecular conformational analysis, vibrational spectra, NBO, HOMO–LUMO and molecular docking of modafinil based on density functional theory, Int. J. Cur. Res. Rev. 10 (2018) 36–45.

[37] D. Sajan, Lynnette Joseph, N. Vijayan, M. Karabacak, Natural and orbital analysis, electronic structure, Non- Linear properties and vibrational spectral analysis of L-histidinium bromide monohydrate : a Density functional theory, Spectrochem. Acta A 81 (2011) 85–98.

[38] S.K. Pathak, R. Srivastava, A.K. Sachan, O. Prasad, L. Sinha, A.M. Asiri, M. Karabacak, Experimental (FT-IR, FT-Raman, UV and NMR) and quantum chemical studies on molecular structure, spectroscopic analysis, NLO, NBO and reactivity descriptors of 3,5-Difluoroaniline, J. Spectrochim. Acta A 135 (2015) 283–295.

[39] Nouar Sofiane Labidi, Non-linear optical properties of substituted hexatriene: AM1 and *ab-initio* quantum chemical calculations, OALIB, J 1 (2014) 1–10.

[40] Anju Linda Varghese, Ignatious Abraham, M. George, DFT studies on nonlinear optical properties of N-[(Naphthalen-5-yl)methyl]-4-Nitrobenzamine, Mater. Today: Proceedings 9 (2019) 92–96.

[41] V. Vidhya, A. Austine, M. Arivazhagan, Quantum chemical determination of molecular geometries and spectral investigation of 4-ethoxy-2, 3-difluoro benzamide, Heliyon 5 (2019), e02365, 1–17.

[42] K. Chaitanya, Molecular structure, vibrational spectroscopic (FT-IR, FT-Raman), UV vis spectra, first order hyperpolarizability, NBO analysis, HOMO and LUMO analysis, thermodynamic properties of benzophenone 2,4-dicarboxylic acid by *ab-initio* HF and density functional method, Spectrochim. Acta 86 (2012) 159–173.

[43] S. Jeyavijayan1, E. Gobinath, J. Senthil Kumar, Structural, spectroscopic investigation and quantum chemical calculation studies of 2,4,6- trimethylphenol for pharmaceutical application, Int. J. Pharmaceut. Sci. Rev. Res. 41 (2016) 214–222.

[44] R. Johnson, Shahar Keinan, Paula Mori-Sánchez, Julia Contreras-García, Aron J. Cohen, Weitao Yang, Revealing noncovalent interactions, J. Am. Chem. Soc. 132 (2010) 6498–6506.

[45] M. Karabacak, E. Kose, E.B. Sas, M. Kurt, A.M. Asiri, A. Atae, DFT Calculations and experimental FT-Raman, NMR, UV-Vis Spectral studies of 3-fluoro Phenylboronic acid, Spectrochem. Acta A 136 (2015) 306–320.

[46] R. Gayathri, M. Arivazhagan, Experimental (FT-IR and FT-Raman) and theoretical (HF and DFT) investigation NMR, NBO, electronic properties and frequency estimation analyses on 2,4,5-trichlorobenzene sulfonyl chloride, Spectrochim. Acta 97 (2012) 311–325.

[47] Gregory K. Pierens, T.K. Venkatachalam, David C. Reutens, NMR and DFT investigations of structure of colchicine in various solvents including density functional theory calculations, Sci. Rep. 7 (2017) 1–9.

[48] Xingya Kang, Shigenori Kuga, Limei Wang, Min Wu, Yong Huang, Dissociation of intra/inter-molecular hydrogen bonds of cellulose molecules in the dissolution process: a mini review, J. Bioresour. Bioprod. 1 (2016) 158–163.

[49] Mihaela Homocianu, Anton Airinei, Intra- inter-molecular interactions-identification and evaluation by optical spectral data in solution, J. Mol. Liq. 225 (2017) 869–876.

[50] K. Arulaabaranam, S. Muthu, G. Mani, S. Sevvanthi, Quantum mechanical computation, spectroscopic exploration and molecular docking analysis of 2-Bromo-4-fluoroacetanilide, J. Mol. Struct. 1220 (2020) 128639.

[51] Zineb Tribak, Mohammed Khalid Skalli, Amal Haoudi, Youssef Kandri Rodi, Omar Senhaji, Experimental approach, computational DFT investigation and a biological activity in the study of an organic heterocyclic compound, Arc. Org. Inorg. Chem. Sci. 4 (2019) 1–7.

[52] Walaa H. Mahmoud, Gehad G. Mohamed, Ahmed M. Refat, Preparation, characterization, biological activity, density functional theory calculations and molecular docking of chelates of diazo ligand derived from M-phenylenediamine and P-chlorophenol, Appl. Organomet. Chem. 37 (2017) 1–19, e3753.

[53] Afroza Zannat, Ajoy Kumer, Md. Nuruzzaman Sarker, Sunanda Paul, The substituent group Activity in the anion of cholinium carboxylate ionic liquids on thermo-physical, chemical reactivity, and biological properties: a DFT study, Int. J. Chem. Technol. 3 (2019) 151–161.

[54] S. Sevvanthi, S. Muthu, M. Raja, S. Aayisha, S. Janani, PES, molecular structure, spectroscopic (FT-IR, FT-Raman), electronic(UV-Vis, HOMO-LUMO), quantum chemical and biological (docking) studies on a potent membrane permeable inhibitor: dibenzoxepine derivative, Heliyon 6 (2020), e04724, 1–16.

[55] Marco L. Lolli, Stefano Sainas, Agnese C. Pippione, Marta Giorgis, Donatella Boschi, Franco Dosio, Use of human dihydroorotate dehydrogenase (hDHODH) inhibitors in autoimmune diseases and new perspectives in cancer therapy, Recent Pat. Anti-Cancer Drug Discov. 13 (2018) 86–105.

[56] Ahmed F. Abdel-Magid, Use of dihydroorotate dehydrogenase inhibitors for treatment of autoimmune diseases and cancer, ACS Med. Chem. Lett. Sep (2020) (In Press).

[57] Kuei-Chung Shih, Chi-Ching Lee, Chi-Neu Tsai, Yu-Shan Lin, Chuan-Yi Tang, Development of a human dihydroorotate dehydrogenase (hDHODH) pharmasimilarity index approach with scaffold-hopping strategy for the design of novel potential inhibitors, PloS One 9 (2014) 1–13, e87960.

[58] Christina Susan Abraham, S. Muthu, Johanan Christian Prasana, Sanja J. Armakovic, Stevan Armakovic, Fathima Rizwana, A.S. Ben Geoffrey, Spectroscopic profiling (FT-IR, FT-Raman, NMR and UV-Vis), autoxidation mechanism (H-BDE) and molecular docking investigation of 3-(4-chlorophenyl)-N, N-dimethyl-3-pyridin-2-ylpropan-1-amine by DFT/TD-DFT and molecular dynamics: a potential SSRI drug, J. Comput. Biol. Chem. (2018) 131–145. https://www.sciencedirect.com/science/journal/14769271/77/supp/C77.

[59] Sebastian Salentin, V. Joachim Haupt, Simone Daminelli, Michael Sch, Polypharmacology rescored: protein-ligand interaction profiles for remote binding site similarity assessment, Prog. Biophys. Mol. Biol. 116 (2014) 174–186.

[60] Yi Fu, Ji Zhao, Zhiguo Chen, Insights into the molecular mechanisms of protein-ligand interactions by molecular docking and molecular dynamics simulation: a case of oligopeptide binding protein, Comput. Math Methods Med. 2018 (2018) 1–12.